Catalytic Activities and Coking Characteristics of Oxides-Supported Ni Catalysts for CH 4 Reforming with Carbon Dioxide

ARTICLE *in* ENERGY & FUELS · MARCH 1998

Impact Factor: 2.79 · DOI: 10.1021/ef970092m · Source: OAI

Catalytic Activities and Coking Characteristics of Oxides-Supported Ni Catalysts for CH_4 Reforming with Carbon Dioxide

Shaobin Wang and G. Q. (Max) Lu*

Department of Chemical Engineering, The University of Queensland, St Lucia 4072, Australia

Received June 2, 1997

Catalytic activities and deactivation characteristics of oxides-supported nickel catalysts for the reaction of methane reforming with carbon dioxide were investigated. The dynamic carbon deposition on various nickel catalysts was also studied by a thermogravimetric method. Among the catalysts prepared, Ni/La_2O_3, $Ni/\alpha\text{-}Al_2O_3$, Ni/SiO_2, and Ni/CeO_2 showed very high CH_4 and CO_2 conversions and moderate deactivation whereas Ni/MgO and Ni/TiO_2 had lower conversions when the Ni reduction was conducted at 500 °C. When Ni/MgO catalyst was reduced at 800 °C, it exhibited not only comparable conversions of CH_4 and CO_2 with other active catalysts but also much longer period of stability without deactivation. The amount of carbon deposited in Ni-based catalysts varied depending on the nature of support and followed the order of Ni/La_2O_3 > $Ni/\alpha\text{-}Al_2O_3$ > Ni/SiO_2 > Ni/MgO > Ni/CeO_2 at 700 °C. The carbons formed on the catalyst surface showed different structural and chemical properties, and these in turn affected the catalytic activity of the catalysts.

1. Introduction

Synthesis gas is now produced mostly by steam reforming of methane. This reaction suffers from severe limitations such as high energy requirement, high H_2/CO product ratio, and poor selectivity for carbon monoxide. Although partial oxidation of methane is free from the above problems, it operates at high temperatures (≥1300 °C) and pressures (up to 150 atm) without catalysts.[1] Besides, the large amount of heat produced in the catalytic reactor is hazardous and difficult to control. Therefore, this approach still has disadvantages. A proposed alternative to steam reforming and oxidative coupling of methane is dry reforming of methane with carbon dioxide.[2] The significance of this reforming reaction is 2-fold: it utilizes CO_2 and methane, two potent greenhouse gases, while it produces syngas, a valuable C_1 chemical feed gas.

Numerous materials have been tested as potential catalysts for reforming of methane with CO_2, while Ni-based catalysts as well as supported noble metal catalysts have been found to have promising catalytic performance.[2−6] However, one of the major problems of this reaction is the deactivation of catalyst caused by carbon formation (or coking) probably via the Boudouard reaction and methane decomposition. It has been reported that supported noble metal catalysts experienced less carbon formation than did Ni-based catalysts.[7−10] Despite this finding, there are still some reports on Ni-based catalysts showing high activity without suffering coking.[11−14] Moreover, nickel-based catalysts deserve more attended research because they are economical industrial catalysts.

It has been observed that the nature of supports affects the catalytic performance of Ni catalysts. The effect of support on the activity of Ni catalysts for reforming methane with CO_2 was first studied by Gadalla and Bower.[15] The catalytic activity, selectivity, and stability of the Ni catalysts varied greatly with different supports such as Al_2O_3, $Al_2O_3-SiO_2$, Al_2O_3-MgO, and Al_2O_3-CaO. They found that Ni on Al_2O_3, Al_2O_3-MgO, and Al_2O_3-CaO resulted in high conversions and the catalysts with supports containing MgO and CaO were most stable. However, catalyst of $Ni/Al_2O_3-SiO_2$ was deactivated rapidly and was shattered. Erdohelyi et al.[16] investigated the catalytic reaction of methane with CO_2 over palladium supported on TiO_2,

* To whom all correspondence should be addressed. Fax: 61 733654199. E-mail: maxlu@cheque.uq.edu.au.

(1) Choudhary, V. R.; Sansare, S. D.; Mamman, A. S. *Appl. Catal.* **1992**, *90*, L1−L5.
(2) Wang, S.; Lu, G. Q.; Millar, G. J. *Energy Fuels* **1996**, *10*, 896−904.
(3) Ross, J. R. H.; van Kenlen, A. N. J.; Hegarty, M. E. S.; Seshan, K. *Catal. Today* **1996**, *30*, 193−199.
(4) Edwards, J. H.; Maitra, A. M. *Fuel Process. Technol.* **1995**, *42*, 269−289.
(5) Shi, J. L.; Zhang, J. Y.; Liu, Z. *Nat. Gas Chem. Eng.* **1995**, *20(2)*, 35−44.
(6) Rostrup-Nielsen, J. R. *Stud. Surf. Sci. Catal.* **1994**, *81*, 25−41.
(7) Richardson, J. T.; Paripatyadar, S. A. *Appl. Catal.* **1990**, *61*, 293−309.
(8) Ashcroft, A. T.; Cheethan, A. K.; Green, M. L. H.; Vernom, P. D. F. *Science* **1991**, *352*, 225−226.
(9) Rostrup-Nielsen, J. R.; Hansen, J. H. B. *J. Catal.* **1993**, *144*, 38−49.
(10) Nakamura, J.; Aikawa, K.; Sato, K.; Uchijima, T. *Catal. Lett.* **1994**, *25*, 265−270.
(11) Yamazaki, O.; Nozaki, T.; Omata, K.; Fujimoto, K. *Chem. Lett.* **1992**, 1953−1954.
(12) Chen, Y. G.; Yamazaki, O.; Tomishige K.; Fujimoto, K. *Catal. Lett.* **1996**, *39*, 91−95.
(13) Zhang, Z. L.; Verykios, X. E. *J. Chem. Soc., Chem. Commun.* **1995**, 71−72.
(14) Ruckenstein, E.; Hu, Y. H. *Appl. Catal.* **1995**, *133*, 149−161.
(15) Gadalla A. M.; Bower, B. *Chem. Eng. Sci.* **1988**, *42*, 3049−3062.

S0887-0624(97)00092-3 CCC: $15.00
Published on Web 01/16/1998

Table 1. Characterization of Catalysts

catalyst	Ni loading (wt %)	support S_{BET} (m^2/g)	catalyst[a] S_{BET} (m^2/g) C	catalyst[a] S_{BET} (m^2/g) R	pore structure	d_1 (nm) reduction	d_2 (nm) reaction
Ni/La_2O_3	4.4	6.4	16.4	19.2	nonporous	15.5	37.5
Ni/SiO_2	4.8	290	239	221	mesoporous	12.0	21.8
Ni/TiO_2	4.6	9.4	8.4	n.d.	mesoporous	27.6	n.d.
Ni/Al_2O_3	5.0	0.8	1.2	3.2	nonporous	31.7	37.5
Ni/MgO	4.9	147.8	55.5	55.7[b]	mesoporous		
Ni/CeO_2	5.3	52	34	29.7	mesoporous		

[a] C, calcined samples; R, reduced samples; u.d., undetected. [b] Reduction at 800 °C.

Al_2O_3, SiO_2, and MgO and observed the order of activity as follows: Pd/TiO_2, Pd/Al_2O_3, Pd/SiO_2, Pd/MgO. However, they did not find significant difference in turnover frequencies of Rh catalysts based on Al_2O_3, SiO_2, TiO_2, and MgO.[17] Takano et al.[18] also worked on Ni catalysts with various supports. The catalytic activity varied depending on the type of support according to the following order, $Al_2O_3 > SiO_2$ with $MgO > SiO_2$. The addition of MgO to SiO_2-supported catalyst increased the catalytic activity but decreased the stability. Rh-supported catalysts (Rh/SiO_2, $Rh/La_2O_3-SiO_2$, and Rh/La_2O_3) were investigated by Gronchi et al.[19] La_2O_3 showed a positive effect on the conversion and selectivity due to its basicity. Zhang et al.[20] studied the effect of carrier and metal particle size on the catalytic activity of Rh in CO_2 reforming of methane. They found that the specific activity of Rh catalyst depended strongly on the carrier employed to disperse the metal, which is related to the carrier acidity. However, Mark and Maier[21] recently reported that there was no appreciable influence of the pore structure or nature of the support on the reaction rate with supported Rh ad Ir catalysts. The influence of the support seemed limited to the stabilization of the metal surface area, which in turn was responsible for catalyst activity.

This work is focused on the investigation of activity of various Ni oxide-supported catalysts and the coking process occurring over these catalysts. We will also study the chemical properties of carbon formed on the supported nickel catalysts so as to elucidate the role of the support on catalyst activity and coking resistivity.

2. Experimental Section

2.1. Catalyst Preparation and Characterization. $Ni(NO_3)_2 \cdot 6H_2O$ (BDH) was used as the precursor for preparation of Ni catalysts. The supports used are α-Al_2O_3 (BDH), SiO_2 gel (Merck), TiO_2 (Merck), MgO (Ajax), La_2O_3 (Fluka), and CeO_2 (BDH). The catalysts were all prepared by the wetness impregnation method, using appropriate nickel nitrate solution at the desired concentration to control the nickel loading at 5% and dried at 103−105 °C for 14 h in air and then calcined at 500 °C for 4 h, also in air.

The BET surface area of catalyst samples was measured using an automated surface area analyzer (NOVA 1200, Quantachrome, USA) with nitrogen as the adsorbate. XRD patterns were obtained with a Philips PW 1840 power diffractometer. Cobalt Kα radiation was employed covering 2θ between 2° and 90°. The mean crystallite diameters were estimated by the Scherrer equation. The XPS measurements were conducted using PHI-560 ESCA system (Perkin-Elmer). All spectra were acquired at a basic pressure of 5×10^{-7} Torr with Mg Kα excitation at 15 kV and recorded in the ΔE = constant mode, pass energy of 50 and 100 eV.

2.2. Catalytic Reaction Experiments. Activity measurements were conducted at 1 atm in a conventional flow system consisting of gas flow controller, a quartz fixed bed reactor, and an on-line gas chromatograph. The quartz reactor (i.d. = 10 mm) was electrically heated. The temperature profile was measured using a thermocouple placed inside the tube with one end centered at the catalyst bed. The reaction products were analyzed using a Shimadzu GC-17A equipped with a TC detector. A carbosphere column was used. The catalysts were reduced in situ in 10%H_2/N_2 flow at 500 °C for 3 h before catalytic testing. For Ni/MgO catalyst a higher reduction temperature was also used. This higher temperature pretreatment was performded at 800 °C for 3 h at 10% H_2/N_2 flow. CO_2 (Matheson) and CH_4 (Matheson) gases were both of ultrahigh purity (>99.995%).

2.3. Thermogravimetric Analysis of Coking. Carbon deposition experiments were carried out on a Shimadzu TGA-50 under atmospheric pressure. A 50 mg sample was placed in a quartz mesh cell (40−100 μm). The calcined samples were first reduced in 10% H_2/N_2 at 800 °C for 2 h and then brought to the reaction temperature of 700 °C under H_2/N_2 flow until the weight reached a constant. The gas stream was then switched to the reactant stream with CO_2:CH_4 = 1:1. The weight change was recorded at 60 s interval by a PC with data acquisition software. The effect of temperature on coking was conducted in a temperature-programmed process. After the sample was reduced at 800 °C for 2 h it was cooled to ambient temperature under H_2/N_2 flow. Then the stream was switched to the mixture of reactants and started each run with the heating rate of 10 °C/min with CO_2:CH_4 = 1:1 at the flow rate of 120 mL/min.

2.4. Temperature-Programmed Oxidation. A 20 mg sample of the used catalyst in the test of fixed-bed reactor was loaded into a Pt pan in TGA and TPO experiments performed in an air flow with the rate of 80 mL/min from ambient temperature to 800 °C at 10 °C/min.

3. Results

3.1. Characterization of the Catalysts. The physical properties of the supports and catalysts are presented in Table 1. It is seen that the surface area of catalysts is generally reduced for those with porous structure supports, as expected, by the impregnation of active phase. However, surface areas of Ni/α-Al_2O_3 and Ni/La_2O_3 catalysts are significantly higher than those of the supports. This is possibly due to pore formation from nickel nitrate decomposition occurring during the

(16) Erdohelyi, A.; Cserenyi, L.; Papp, E.; Solymosi, F. *Appl. Catal.* **1994**, *108*, 205−219.
(17) Erdohelyi, A.; Cserenyi, L.; Solymosi, F. *J. Catal.* **1993**, *141*, 287−299.
(18) Takano, A.; Tagawa T.; Goto, S. *J. Chem. Eng. Jpn.* **1994**, *27*, 723−731.
(19) Gronchi, P.; Mazzocchia, C.; Rosso, R. D. *Energy Convers. Mgmt.* **1995**, *36*, 605−608.
(20) Zhang, Z. L.; Tsipouriari, V. A.; Efstathiou, A. M.; Verkykios, X. E. *J. Catal.* **1996**, *158*, 51−63.
(21) Mark M. F.; Maier, W. F. *J. Catal.* **1996**, *164*, 122−130.

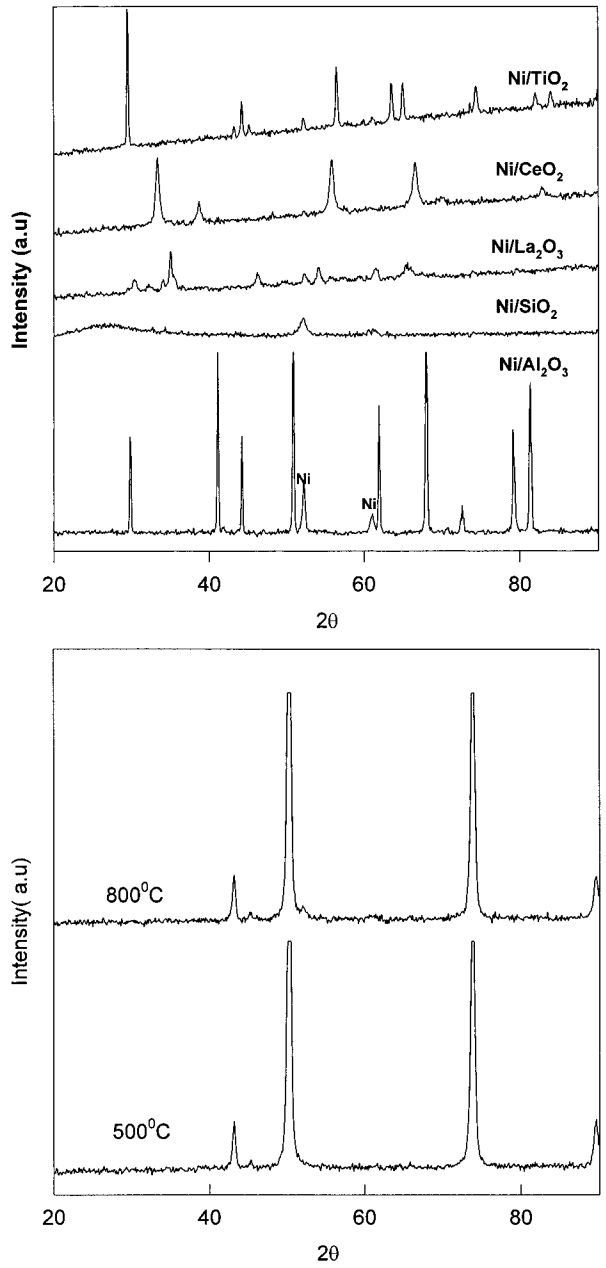

Figure 1. XRD patterns of Ni catalysts after reduction: (a, top) the XRD patterns of Ni catalysts reduced at 500 °C; (b, bottom) XRD patterns for Ni/MgO reduced at 500 and 800 °C.

calcination and reduction steps.[22] In addition, impregnation of active phase on nonporous support may develop the interlayer between the support and active phase resulting in larger surface area of the catalyst.

The XRD patterns of the reduced catalysts are shown in Figure 1, a and b. For Ni/α-Al_2O_3, Ni/La_2O_3, Ni/SiO_2, and Ni/TiO_2 catalysts the nickel peaks are clearly demonstrated in their XRD spectra while no nickel diffraction peaks appear in XRD spectra of Ni/CeO_2 (Figure 1a) and Ni/MgO catalysts (Figure 1b) at 500 °C reduction. From the peak width the nickel crystallite size was obtained and the results are given in Table 1. The nickel particle size depends on the support porosity and the metal−support chemical interaction. For Ni/α-Al_2O_3 and Ni/TiO_2, the lower porosity of the supports resulted in less dispersion of metal and thus larger particle size. The well-developed porosity of SiO_2 led to higher dispersion of nickel particles and smaller particle size. Although La_2O_3 has nonporous structure, nickel particle size of Ni/La_2O_3 is less than that of Ni/TiO_2 and Ni/Al_2O_3 catalysts and similar to that of Ni/SiO_2. This is probably due to the nature of the support, La_2O_3. It is known that La_2O_3 has higher ability to disperse metal crystallites on supports and is usually used as a promoter for oxide-supported catalysts. The reduction of Ni/MgO is hindered because the formation of solid solution of NiO−MgO in which the Ni^{2+} ions are included in MgO matrix.[14,23] Therefore, it is difficult to be reduced and nickel particle cannot be detected in XRD measurement at 500 °C reduction. The XRD pattern of Ni/MgO catalyst prereduced at 800 °C (Figure 1b) shows a shoulder peak of nickel reflectance peak. This indicates that higher temperature reduction at 800 °C could produce nickel crystallites on Ni/MgO catalyst. The absence of nickel diffraction peaks in XRD pattern of Ni/CeO_2 catalyst is probably due to the well dispersion of nickel particle on CeO_2 and the reductive behavior of CeO_2 support.

Table 2. Surface Composition of Nickel Catalysts before and after Reaction[a]

catalyst	treatment	C (%)	O (%)	Ni (%)	La, Al, Si, Ce, Mg (%)
Ni/La_2O_3	reduced	23.1	53.0	2.1	21.8
	reaction	94.7	4.4	4.4	1.4
Ni/MgO	reduced	11.9	50.3	0.8	37.0
	reaction	29.0	40.8	0.4	29.8
Ni/Al_2O_3	reduced	10.1	60.6	9.7	19.6
	reaction	77.2	15.9	0.6	6.4
Ni/SiO_2	reduced	3.1	66.5	0.8	29.6
	reaction	17.7	56.4	56.4	25.8
Ni/CeO_2	reduced	17.3	53.8	2.8	26.1
	reaction	45.2	40.2	2.4	12.2

[a] Reaction conditions: CO_2/CH_4 = 1:1, P = 1 atm, T = 700 °C.

The surface properties of fresh catalysts are analyzed by the XPS technique, and the chemical compositions of different elements and C 1s spectra are shown in Table 2 and Figure 2, respectively. The C 1s peaks on all catalysts appear at the higher binding energy (>290 eV), indicating the presence of surface carbonate (CO_3^-) species. The surface carbonate species is expected to be formed due to the interaction of CO_2 from the atmosphere. The carbonate content on the catalyst surface may be related to the acidity−basicity property of the catalyst. From the data in Table 2 it is found that carbonate on Ni/La_2O_3 is highest which may be indicative of its highest basic property.

3.2. Catalytic Activity and Stability. The CH_4 and CO_2 conversions in CO_2/CH_4 reaction on various Ni-based catalysts in the temperature range of 500−800 °C are shown in Figure 3. It is apparent that Ni/La_2O_3, Ni/Al_2O_3, and Ni/SiO_2 have higher conversions than Ni/TiO_2 and Ni/MgO. Ni/CeO_2 catalyst shows comparable conversion at 500−700 °C to other catalysts such as Ni/La_2O_3, Ni/Al_2O_3, and Ni/SiO_2. Above 700 °C the CH_4 and CO_2 conversions tend to level off. In the case of Ni/TiO_2, catalyst conversions generally increase up to 600 °C and then decrease which suggests that this

(22) Halliche, D.; Bouarab, R.; Cherifi, O.; Bettahar, M. M. *Catal. Today* **1996**, *29*, 373−377.

(23) Hu, Y. H.; Ruchenstein, E. *Catal. Lett.* **1996**, *36*, 145−149.

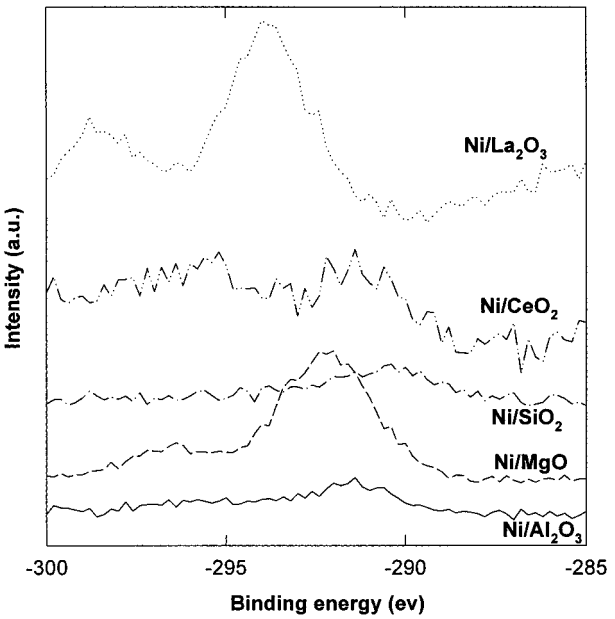

Figure 2. C 1s spectra of various Ni catalysts before reaction.

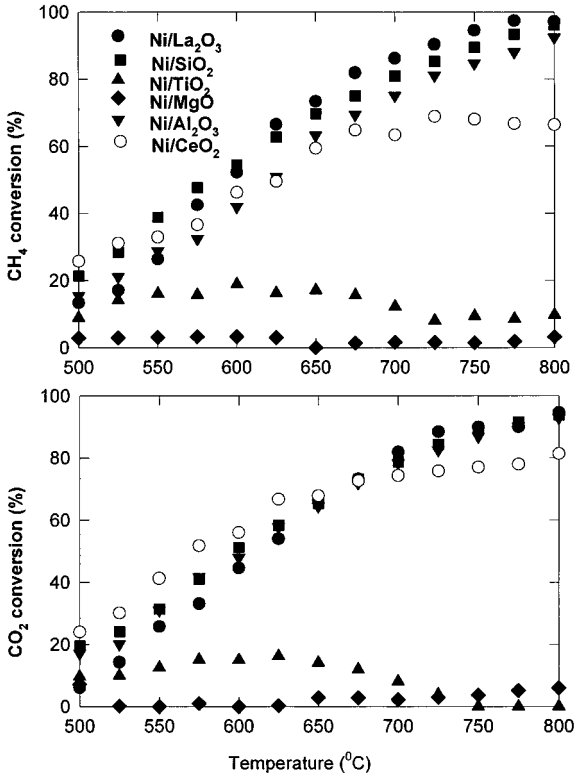

Figure 3. CH_4 and CO_2 conversions at different temperatures. Reaction conditions: $CO_2/CH_4 = 1:1$, $P = 1$ atm.

catalyst showed quick deactivation. Swaan et al.[24] reported that Ni/TiO_2 catalyst completely deactivated at 400 °C within 1 h of testing. Their results are similar to what we found in this investigation. Ni/MgO first had some activity at 500 °C and then showed little conversion of CH_4 or CO_2 until the temperature reached 800 °C. However, the conversion is only about 5%. This indicates that Ni/MgO catalyst if reduced at 500 °C has little activity for CO_2 reforming of methane.

(24) Swaan, H. M.; Kroll, V. C. H.; Martin, G. A.; Mirodatos, C. *Catal. Today* **1994**, *21*, 571−578.

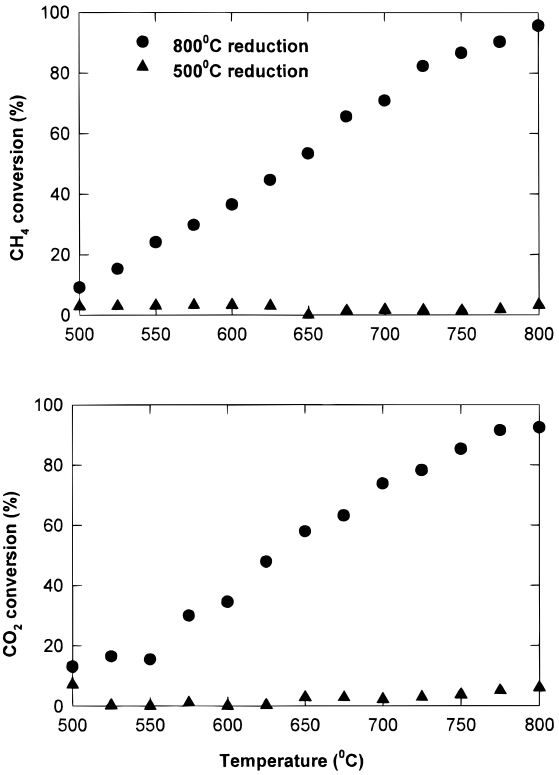

Figure 4. Conversions of CH_4 and CO_2 on Ni/MgO catalysts reduced at different temperature. Reaction conditions: $CH_4/CO_2 = 1:1$, $P = 1$ atm.

There are some reports showing that Ni/MgO catalyst had high activity and demonstrated a long-term stability for the reaction of CH_4 reforming with CO_2, but to activate the catalyst much higher temperature was required.[11,14] Yamazaki et al. [11] reported that Ni/MgO catalyst treated in hydrogen stream at 850 °C showed higher activity than that of Ni/CaO−MgO but less stability because of higher coking. The latter could keep its activity as long as 3 days. Ruckenstein and Hu[14] also found that Ni/MgO catalyst reduced at 790 °C exhibited over 90% conversions of CH_4 and CO_2 at the same temperature and remained unchanged during 120 h. However, for unreduced Ni/MgO catalyst, the CH_4 and CO_2 conversions were about 5%. Figure 4 shows the conversions of CH_4 and CO_2 on Ni/MgO catalyst reduced at 800 °C for 3 h. The results show that Ni/MgO catalyst has high activity if properly pretreated in H_2. The CH_4 or CO_2 conversion can reach 90% at 800 °C comparable to other active catalysts such as Ni/La_2O_3, Ni/Al_2O_3, and Ni/SiO_2. These observations are similar to the results reported by Ruckenstein and Hu.[14]

The deactivation testing was performed at 700 °C over Ni-based catalysts except for Ni/TiO_2 and the results are presented in Figure 5. For Ni/MgO catalyst reduction was conducted at 800 °C. As can be seen, the long-term stability of Ni/MgO catalyst is the best among the five catalysts and it exhibits essentially no deactivation under the condition employed in this test. For Ni/La_2O_3 catalyst, CH_4 conversion increases first and then decreases after 1 h, suggesting deactivation occurred. However, after a certain period of time (5 h) the deactivation becomes much less significant. This result is similar to that reported by Swaan et al.,[24] but unlike

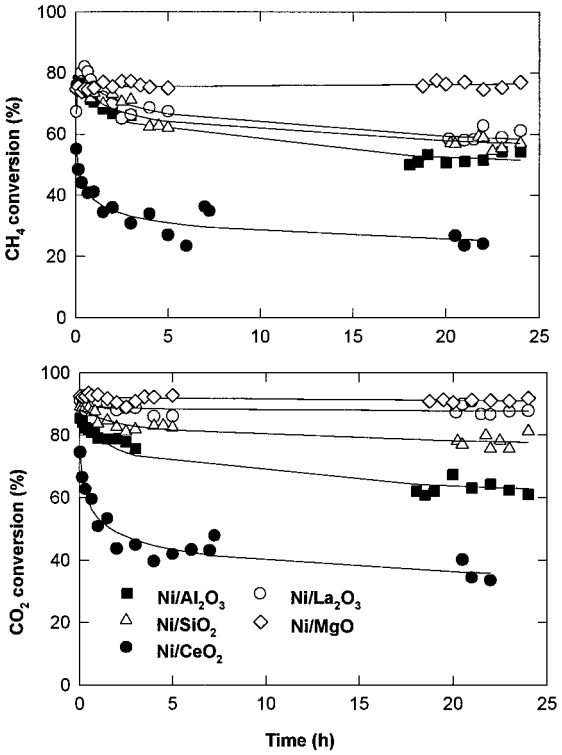

Figure 5. Catalyst deactivation versus time at 700 °C. Reaction conditions: $CH_4/CO_2 = 1:1$, $P = 1$ atm.

Table 3. Deactivation Characteristics of Nickel-Based Catalysts[a]

catalyst	$conv_{3\ h}/conv_{10\ min}$	carbon deposition (g of C/g of cat.)	R_{d_2/d_1}
Ni/CeO_2	0.65	0.02	
Ni/Al_2O_3	0.72	0.15	1.2
Ni/SiO_2	0.87	0.068	1.8
Ni/La_2O_3	0.97	0.48	2.4
Ni/MgO	1.1	0.049	

[a]Reaction conditions: $CO_2/CH_4 = 1:1$, $P = 1$ atm, $T = 700$ °C.

the report by Zhang and Verykios.[25] They found that Ni/La_2O_3 catalyst showed a much lower initial activity and increasing activity at about 1−5 h and after that the activity kept stable and no deactivation was observed. Ni/CeO_2 shows much higher initial deactivation than other catalysts. After 5 h the conversion of CH_4 decreases from 60% to 25%. Ni/Al_2O_3 and Ni/SiO_2 catalysts show moderate deactivation during the 24 h testing. After 24 h, CH_4 conversion for Ni/Al_2O_3 and Ni/SiO_2 catalysts decreased from initial 77% and 75% to 50% and 57%, respectively.

The deactivation rates of various supported nickel catalysts are quantified by calculating the ratio of CH_4 conversion after 3 h on stream over that after 10 min on stream. The deactivation characteristics are shown in Table 3. It is seen that the conversion is only about 65% of the initial conversion for Ni/CeO_2 catalyst while the conversions after 3 h were reduced by 28% and 13% for Ni/Al_2O_3 and Ni/SiO_2 catalysts, respectively. In contrast, the decreases in CH_4 conversion over both Ni/La_2O_3 and Ni/MgO catalysts are little. The deactivation rates of these catalysts show the following order: $Ni/CeO_2 > Ni/Al_2O_3 > Ni/SiO_2 > Ni/La_2O_3 > Ni/MgO$.

(25) Zhang, Z. L.; Verykios, X. E. *Appl. Catal.* **1996**, *138*, 109−133.

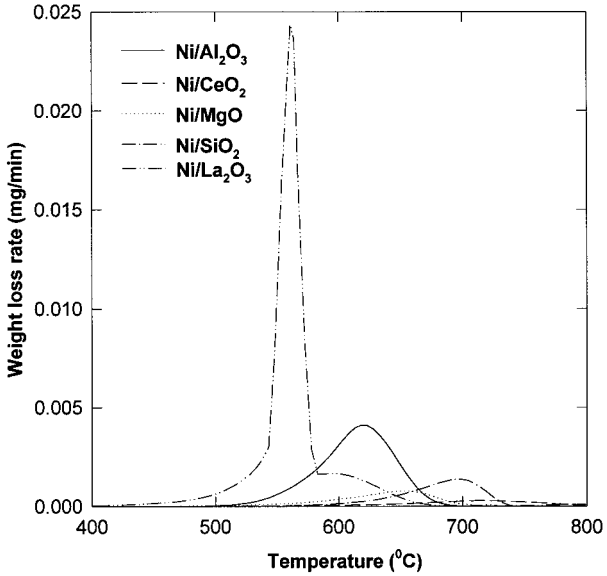

Figure 6. TPO profiles of carbonaceous species formed on catalyst after reaction at 700 °C for 24 h.

Table 4. Activation Energies for Carbon Oxidation on Used Catalysts

catalyst	temp (°C)	E_a (kJ/mol)
$Ni/\alpha\text{-}Al_2O_3$	500−700	260
Ni/SiO_2	500−725	201
Ni/MgO	500−720	148
Ni/La_2O_3	400−700	164
Ni/CeO_2	500−720	112

To characterize the amount of carbon deposits on used catalysts and their activities, TPO experiments were carried out using a TGA. The amount of carbon on catalyst after 24 h reaction at 700 °C determined by TPO is listed in Table 3. It is seen that Ni/CeO_2 catalyst has the least amount of deposited carbon whereas Ni/La_2O_3 has the highest carbon content (about 50%). Carbon deposits on Ni/SiO_2 and Ni/MgO catalysts are less than 10%. The order of coking on catalyst follows the order $Ni/La_2O_3 > Ni/Al_2O_3 > Ni/SiO_2 > Ni/MgO > Ni/CeO_2$.

The TPO profiles of deposited carbon on catalysts after 24 h reaction on stream at 700 °C are showed in Figure 6. TPO profile of the carbon on Ni/La_2O_3 catalyst is quite different from those on other catalysts. There are two peaks occurring at about 550 and 600 °C for Ni/La_2O_3 catalyst, which indicates that two types of carbons formed on Ni/La_2O_3 catalyst. It is noted that the temperature of maximum oxidation differs among catalysts. The oxidation peak of carbon on $Ni/\alpha\text{-}Al_2O_3$ catalyst is centered at 620 °C. For Ni/MgO catalyst, the temperature of maximum oxidation occurs at 650 °C; for Ni/SiO_2 and Ni/CeO_2, especially for Ni/CeO_2, the temperatures are higher and appear at about 700 and 750 °C. The above results demonstrate that carbons on different catalysts show different oxidation activities thus affecting the catalytic activities and deactivation of these catalysts. From the TPO profiles, activation energies of carbon oxidation on different supports were calculated (Table 4) by

$$dX/dT = Ae^{-E_a/RT}(1 - X) \qquad (1)$$

where $X = (W_0 - W)/(W_0 - W_f)$, W_0 is the initial weight,

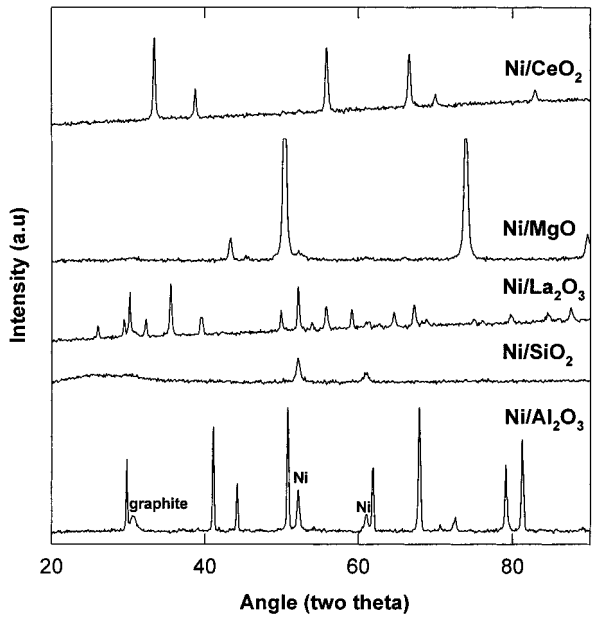

Figure 7. XRD patterns of Ni catalysts after reaction at 700 °C for 24 h.

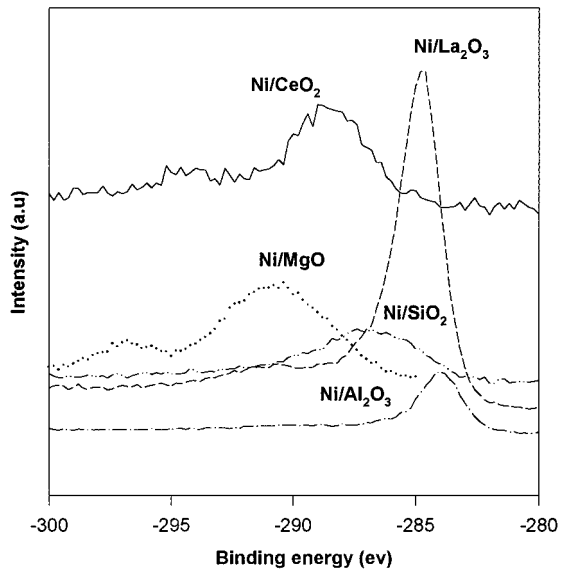

Figure 8. Comparison of C 1s profiles on various catalysts after CO_2/CH_4 reforming reaction at 700 °C for 24 h.

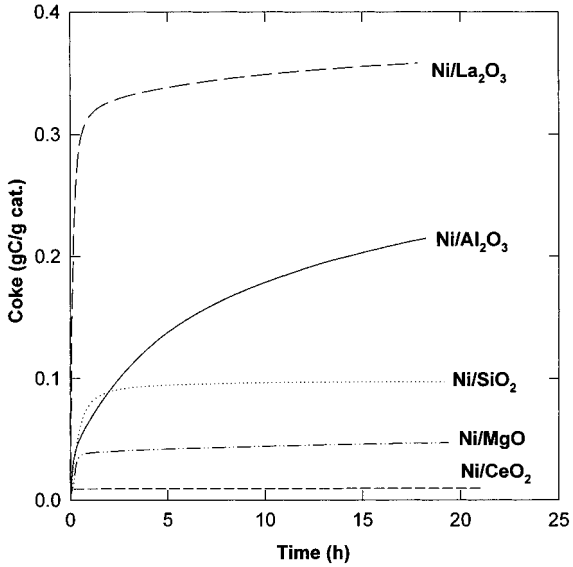

Figure 9. TGA profiles of coking on Ni catalysts at 700 °C. Reaction conditions: $CO_2/CH_4 = 1;1$, $P = 1$ atm.

W is the weight remaining, and W_f is the weight at the end of the TPO reaction. It is found that the oxidation reaction is of the first order. The activation energies for carbon oxidation on Ni/MgO, Ni/La_2O_3, and Ni/CeO_2 catalysts are lower while they are much higher for Ni/α-Al_2O_3 and Ni/SiO_2. This indicates that carbon deposits formed on Ni/MgO and Ni/CeO_2 are more active for gasification. Although the amount of carbon on Ni/La_2O_3 is higher, they show greater activity for gasification, which can explain the higher catalytic activity in CO_2 reforming reaction. For Ni/α-Al_2O_3 and Ni/SiO_2 catalysts, less activity of the carbon deposits leads to accumulation of coke on catalysts.

The XRD spectra of used catalyst are shown in Figure 7. It is seen that sharp peaks of Ni diffraction are seen in the XRD spectra of Ni/La_2O_3, Ni/SiO_2, and Ni/α-Al_2O_3 catalysts and a shoulder peak for Ni crystallite reflection in Ni/MgO catalyst. Nickel particle size was calculated for these catalysts and the results are shown in Table 1. Nickel crystallite size of the used catalyst is generally increased indicating that sintering of catalyst occurred in the tested catalysts except for Ni/CeO_2 catalyst. The degree of sintering is significant for Ni/La_2O_3 and Ni/SiO_2 catalysts. However, it is not so appreciable for Ni/α-Al_2O_3 catalyst (Table 3).

The XRD analyses on used catalysts show the presence of two distinct species of carbon on catalysts (Figure 7). In XRD spectra of the used Ni/Al_2O_3 and Ni/La_2O_3 catalysts, a sharp peak of graphitic carbon appears. For Ni/MgO and Ni/SiO_2 catalyst the carbon peak is weak and broad which is indicative of amorphous carbon species. However, no carbon peak can be detected on the used Ni/CeO_2 catalyst. This is due to the low carbon deposition, which can be seen from the TPO results (Table 3) and coking studies (Figure 9).

The surface compositions of the used catalysts determined by XPS measurements are shown in Table 2. The results indicate that the surface carbon is the dominant element on used Ni/La_2O_3 and Ni/Al_2O_3 catalysts. Nickel on Ni/La_2O_3 and Ni/SiO_2 catalysts cannot be detected. Much less nickel exists on the surface of Ni/α-Al_2O_3 catalyst. This is mainly because of the coverage of carbonaceous species on the surface of used catalysts. It is noted that the surface carbon on Ni/CeO_2 catalyst is much higher than that on Ni/MgO and Ni/SiO_2 catalyst. This may be due to its high basicity resulting in more carbonate species absorbed on its surface. This is reflected in the C 1s spectra (Figure 8). Comparison of C 1s spectra of different catalysts reveals that the main carbonaceous species on the surface of used Ni/La_2O_3 and Ni/α-Al_2O_3 catalysts is mainly graphitic carbon, which is much different from those on the fresh catalysts. The peaks of maximum carbon signal on used Ni/CeO_2 and Ni/SiO_2 catalysts are also shifted on the binding energy scale. The main carbonaceous species are in the form of $-CO-C-$ and CO_3^-. However, the signal maximum of C 1s on used Ni/MgO catalyst did not show shift though the amount of carbon was increased.

3.3. Carbon Deposition. Coking profiles on various catalysts at 700 °C are shown in Figure 9. It is seen

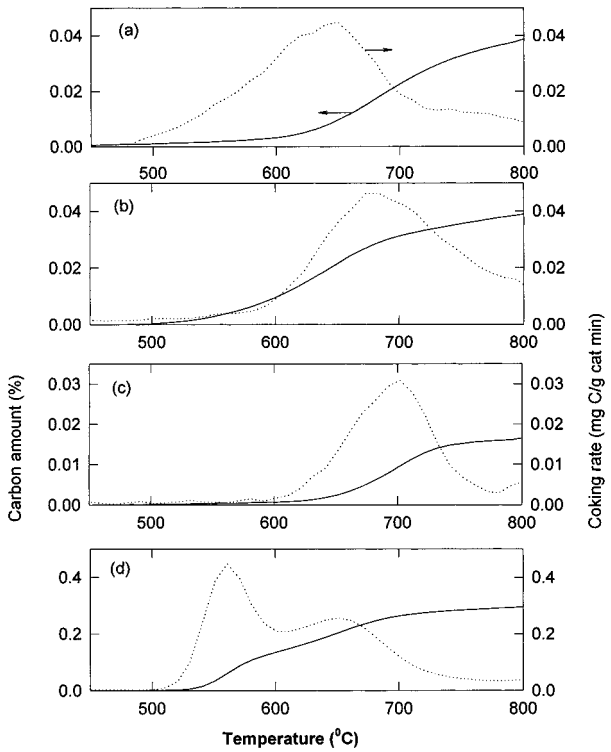

Figure 10. TGA profiles of coking during a temperature program process. Reaction conditions: $CO_2/CH_4 = 1:1$, $P = 1$ atm. (a) Ni/α-Al_2O_3, (b) Ni/SiO_2, (c) Ni/MgO, (d) Ni/La_2O_3.

that coking profiles show a similar trend. However, the amount of coke on various catalysts varies to a great extent. The coke formation is much faster in the beginning stage, but after half an hour a slower coking is observed. Coking on Ni/La_2O_3, Ni/SiO_2, Ni/MgO, and Ni/CeO_2 catalysts tends to level off after 1−2 h. However, coking on Ni/α-Al_2O_3 catalyst increases until 20 h. Coking amount on Ni/La_2O_3 catalyst is about 35 times of that on Ni/CeO_2 catalyst. The coking order is Ni/La_2O_3 > Ni/Al_2O_3 > Ni/SiO_2 > Ni/MgO > Ni/CeO_2. It is noted that this order is the same as that found by the deactivation tests in the fixed bed reactor.

Coking profiles in a temperature-programmed process on nickel-based catalysts are shown in Figure 10. It is seen that all coking profiles show similar patterns. The carbon formation can be divided into three stages, namely (1) induction period, (2) acceleration in coking rate, and (3) decrease in coking rate. It is also seen that carbon deposition on Ni/La_2O_3 is quite different from that on the other three catalysts. TPC spectra of Ni/La_2O_3 exhibit two peaks at 560 and 650 °C, respectively. TPC spectra of Ni/α-Al_2O_3, Ni/SiO_2, and Ni/MgO catalysts show only one peak centered at 650, 680, and 700 °C, respectively. In Figure 10 it is also seen that coking begins at 500 °C on Ni/La_2O_3 and Ni/α-Al_2O_3 catalysts whereas coking rate is very slow at 500−600 °C and increases quickly after 600 °C on Ni/SiO_2 and Ni/MgO catalysts.

The activation energies can be calculated using the coking rate curves. The rate of carbon formation can be expressed as

$$R_c = \mathrm{d}(W/W_0)/\mathrm{d}T = k_c f_c(t) \qquad (2)$$

where k is constant, W_0 is W at the temperature when coking begins, and $f(t)$ is a function of temperature. If we employ the zero model for coking, $f_c(t)$ is a constant and k_c can be replaced by the Arrhenius equation $k = k_0 \exp(-E_a/RT)$. Thus we have

$$\ln\frac{\mathrm{d}(W/W_0)}{\mathrm{d}T} = \ln k_0 - \frac{E_0}{RT} \qquad (3)$$

If we plot $\ln[\mathrm{d}(W/W_0)/\mathrm{d}T]$ vs $1/T$, the activation energy can be obtained (Table 5). It is seen that activation energy for coking on Ni/α-Al_2O_3 is the lowest, which reflects the higher coking activity of this catalyst. The activation energies for Ni/α-Al_2O_3, Ni/SiO_2, and Ni/MgO catalysts follow the order Ni/α-Al_2O_3 > Ni/SiO_2 > Ni/MgO. It is noted that the activation energy for coking on Ni/La_2O_3 at the induction stage is much higher. After that it became low resulting in easier coking occurring on Ni/La_2O_3. Rudnitskii et al.[26] calculated the activation energy for coking on Ni/Al_2O_3 to be 100 kJ/mol which is close to our value for Ni/Al_2O_3.

Table 5. Activation Energies for Coking on Ni Catalysts

catalyst	temp (°C)	E_a (kJ/mol)	temp (°C)	E_a (kJ/mol)
Ni/α-Al_2O_3	510−630	108	640−790	89
Ni/SiO_2	530−670	150	680−790	90
Ni/MgO	570−690	271	700−780	278
Ni/La_2O_3	490−560	467	570−610	124
	610−650	39	660−770	190

4. Discussion

4.1. Effect of Support on Catalytic Activity and Stability. In this work we have shown that catalytic activities of various nickel-based catalysts in terms of CH_4 and CO_2 conversions are influenced by the metal crystallite size, support properties, and metal−support interaction. Among the catalysts, Ni/La_2O_3, Ni/SiO_2, Ni/α-Al_2O_3, and Ni/CeO_2 catalysts have high activities, while Ni/MgO and Ni/TiO_2 catalysts showed much lower activities. However, Ni/MgO catalyst, if reduced at high temperature (800 °C) showed comparable conversion to other four active catalysts. This result is very similar to that reported by Swaan et al.[24] They observed similar activity for Ni/SiO_2 and Ni/La_2O_3 and 5% conversion for Ni/MgO at 550 °C and Ni/TiO_2 at 400 °C. The stability testing showed that no deactivation was observed for Ni/MgO catalyst after 24 h reaction at 700 °C, while other catalysts showed varied deactivation in which the deactivation rate for Ni/CeO_2 catalyst was highest.

For Ni/La_2O_3, Ni/SiO_2, and Ni/α-Al_2O_3 catalysts the high catalytic activity can be attributed to the high metal dispersion and/or less metal−support interaction, though they have high coking ability. In the study of the temperature effect on reforming reaction, it is found that CH_4 and CO_2 conversions are higher on Ni/SiO_2 catalyst than those on Ni/La_2O_3 and Ni/α-Al_2O_3 catalysts at lower temperatures. This can be related to the variation in the metal dispersion in their respective fresh catalysts. As the temperature increases, Ni/La_2O_3 catalyst shows higher activities than those of Ni/SiO_2 and Ni/α-Al_2O_3 catalysts. This is contradictory to the highest carbon accumulation found in this work. Higher

(26) Rudnitskii, L. A.; Solbleva, T. N.; Korotkova, G. G.; Alekseev, A. M. *Natl. Meeting Am. Chem. Soc. (Pet. Chem.)* **1995**, 567−569.

activity of Ni/La_2O_3 must be attributed to the development of new active sites including carbon species.

Zhang and Verykios[25] reported that Ni/La_2O_3 catalyst showed high stability because a new reaction pathway occurred at the Ni/La_2O_3 interface. They proposed a mechanism that under the CH_4/CO_2 reaction condition, CH_4 mainly cracks on the Ni crystallites to form H_2 and surface carbon species (CH_x species), while CO_2 preferably absorbs on the La_2O_3 support or the LaO_x species which are decorating the Ni crystallites in the form of $La_2O_2CO_3$. At high temperatures the oxygen species of $La_2O_2CO_3$ may participate in reactions with the surface carbon species (CH_x) on the neighboring Ni sites to form CO. Due to the existence of such synergetic sites which consist of Ni and La elements, the carbon species formed on the Ni sites are favorably removed by the oxygen species originated from $La_2O_2CO_3$, thus resulting in an active and stable performance.

The higher catalytic activity and stability of Ni/SiO_2 catalyst as compared to that of Ni/Al_2O_3 catalyst can be ascribed to several reasons: (1) porous structure of support; (2) higher dispersion of active Ni crystallite; and (3) less coking ability. It has been found that the support with porous structure has higher activity for the reaction of methane reforming with CO_2.[27] The active component in porous support can easily diffuse into the inner pores of the support resulting in high dispersion and more active sites. In addition, high porosity increases the amount of contact that the gas has with the catalyst surface thus leading to high conversion and longer life of the catalyst. In particular, in this reaction lower coking rate of Ni/SiO_2 prevents the blockage of the porous structure and therefore maintains high activity of the catalyst for longer period of time.

For the Ni/MgO catalyst, formation of NiO and MgO solid solution makes the activation of this catalyst difficult. Our investigation has demonstrated that Ni/MgO catalyst reduced at 500 °C has little activity, which means that reduction pretreatment at 500 °C could not activate the catalyst. This is because of the formation of NiO and MgO solid solution, and the results are similar to that reported by Bradford and Vannice.[28] The formation of NiO/MgO solutions has the following consequences:[14,23] (i) only a small amount of NiO is reduced to Ni which segregates as small particles on the surface of the support and little sintering occurs; (ii) because there are strong interactions between the small Ni particles on the reduced Ni/MgO catalyst, the electron donor ability (Lewis basicity) of Ni is decreased. The bonding of CO molecule to Ni is weakened, and thus the ability for disproportionation of CO is decreased. It is generally known that nickel crystallite is the active site for reforming of methane with carbon dioxide. XRD measurements indicated that NiO could not be reduced to nickel metal until 800 °C. Therefore, Ni/MgO catalyst shows little activity after 500 °C reduction while higher temperature pretreatment activated Ni/MgO, and it shows little sintering and coking.

In the case of Ni/TiO_2 there exists a strong metal and support interaction (SMSI) which affects the catalytic activity. Some researchers have shown that high temperature and prolonged reduction of Ni/TiO_2 cause the increase in TiO_x coverage due to immigrating from the TiO_2 carrier to block the reduced nickel sites responsible for catalytic activity.[25,29] Swaan et al. [24] reported that a Ni/TiO_2 catalyst completely deactivated at 400 °C within an hour on stream because it was reduced at much higher temperature (700 °C). Activity of Ni/TiO_2 catalyst was examined at 600 °C.[28] The Ni/TiO_2 catalyst exhibited a gradual deactivation due to additional site blockage induced by immigrating TiO_x and particle sintering. Ruckenstein and Hu[30] also reported that CO initial yield on Ni/TiO_2 catalyst is relatively small and decreases quickly with time. The lower yield and fast decay with time is also due to SMSI phenomenon and carbon deposition.

For the Ni/CeO_2 catalyst, the strong metal−support interaction is also the main factor influencing the catalyst activity.[31,32] However, this SMSI in Ni/CeO_2 is little understood at present. For this reforming reaction the typical SMSI, as occurred in Ni/TiO_2, causing a partial coverage of the metal by CeO_x suboxides may be partially responsible for the low catalytic activity. In addition, some researches have found that methyl radicals produced by the decomposition of hydrocarbons react extensively with CeO_2 leading to their conversion to total oxidation product like CO_2.[33,34]

4.2. Carbon Formation and Its Chemical Properties. The deposited carbon on catalyst during methane reforming may be from either methane decomposition or carbon monoxide disproportionation (Boudouard reaction).[2]

$$CH_4 \rightarrow C + 2H_2 \quad (4)$$

$$2CO \rightarrow CO_2 + C \quad (5)$$

Swaan et al.[24] using isotope labeling and TPO techniques revealed that carbon deposits formed on the Ni/SiO_2 catalyst during CH_4/CO_2 reforming at 700 °C originated from both CH_4 and CO_2. Decomposition is not the dominant carbon formation mechanism. Goula et al.[35] studied the relative proportion of reaction routes that lead to carbon formation by various transient techniques and found that two kinds of carbon species mainly accumulated on the surface of $Ni/CaO-Al_2O_3$ catalyst, whereas the amount, origin, and their reactivity strongly depended on the support composition. Bradford and Vannice[28] reported that their TPO results suggested that carbon monoxide disproportionation is a likely mechanism for carbon deposition during CH_4/CO_2 reforming. However, the results of Tavares er al.[36] and Chesnokov et al.[37] on carbon deposits by microscopic

(27) Wang S.; Lu, G. Q. *Appl. Catal.*, submitted for publication.
(28) Bradford M. C. J.; Vannice, M. A. *Appl. Catal.* **1996**, *142*, 73−96.
(29) Takatani S.; Chung, Y. W. *J. Catal.* **1984**, *90*, 75−85.
(30) Ruckenstein, E.; Hu, Y. H. *J. Catal.* **1996**, *162*, 230−238.
(31) Trovarelli, A. *Catal. Rev. Sci. Eng.* **1996**, *38*, 439−520.
(32) Badri, A.; Binet, C.; Lavalley, J.-C. *J. Chem. Soc., Faraday Trans.* **1996**, *92*, 1603−1608.
(33) Campbell, K. D.; Zhang, H.; Lunsford, J. H. *J. Phys. Chem.* **1988**, *92*, 750−753.
(34) Tong, Y.; Rosynek, M. P.; Lunsford, J. H. *J. Phys. Chem.* **1989**, *93*, 2896−2898.
(35) Goula, M. A.; Lemonidou, A. A.; Efstathiou, A. M. *J. Catal.* **1996**, *161*, 626−640.
(36) Tavares, M. T.; Alstrup, I.; Berrisrdo, C. A.; Rostrup-Nielsen, J. R. *J. Catal.* **1994**, *147*, 525−534.
(37) Chesnokov, V. V.; Zaikovskii, V. I.; Buyanov, R. A.; Molchanov, V. V.; Plyasova, L. M. *Catal. Today* **1995**, *24*, 265−267.

study suggested that methane decomposition is the main route responsible for carbon deposition. Our calculation has shown that at low temperature (<700 °C) the CO disproportionation is the main mechanism of carbon deposition while at high temperature (>700 °C) the CH_4 decomposition constitutes the main mechanism[2]. Therefore, carbon deposition process is strongly influenced by the nature of a support and temperature.

TPC spectra of Ni/La_2O_3 show two peaks (Figure 10) which may indicate that two mechanisms are involved in the carbon formation. Based on the thermodynamic calculation it is deduced that at 500−600 °C CO disproportionation dominates the carbon formation while at the temperature range of 600−800 °C CH_4 dissociation will be the main cause of carbon deposition on Ni/La_2O_3 catalyst. For Ni/Al_2O_3, Ni/SiO_2, and Ni/MgO catalysts it is also concluded that carbon from CO disproportionation is small before 700 °C, and CH_4 decomposition is the main route for carbon deposits.

It has been suggested that catalyst support influence the coke resistivity of nickel catalyst via stabilization of different CH_x surface intermediates. Osaki et al.[38] used pulse surface reaction rate analysis to study CH_4/CO_2 reforming and found that the more hydrogen-deficient CH_x led to more carbon deposition. The values of the number of hydrogen in CH_x were as follows: $x = 2.7$ for Ni/MgO, 2.4 for Ni/Al_2O_3, 1.9 for Ni/TiO_2, and 1.0 for Ni/SiO_2. Accordingly, Ni/MgO is therefore more resistant to coking than Ni/Al_2O_3 and Ni/SiO_2, which is consistent with the results in this study. For Ni/Al_2O_3 and Ni/SiO_2, CO TPD studies showed that at lower Ni loadings, Ni/SiO_2 absorbs much less CO than Ni/Al_2O_3.[30] This probably explained the less coking on Ni/SiO_2 catalyst found in this work.

In this study, it has been observed that catalyst support also has an important effect on the chemical properties of the deposited carbon. Carbon deposits on various nickel-based catalysts have different structure and reactivity. XRD spectra have shown that two types of carbon, graphitic and amorphous, are formed on Ni catalysts (Figure 7). XPS measurements also showed that two major carbonaceous species (graphite and carbonate) are found on the surface of used catalysts (Figure 8). Hence, it is deduced that the amorphous carbon on catalyst has the structure of carbonate. Carbon on Ni/La_2O_3 and $Ni/\alpha\text{-}Al_2O_3$ catalysts is mainly in the form of graphite, while on Ni/MgO, Ni/SiO_2, and Ni/CeO_2 catalysts carbon is accumulated as amorphous carbonate.

Carbon species on nickel catalyst from CH_4/CO_2 reaction has different oxidation reactivities. TPO profiles indicated that carbon deposited on $Ni/\alpha\text{-}Al_2O_3$ and Ni/La_2O_3 catalysts could be easily oxidized, whereas the ones on Ni/MgO, Ni/SiO_2, and Ni/CeO_2 catalysts reacted at only high temperatures, indicative of less oxidation reactivity. Therefore, it can be concluded that graphitic carbon is more reactive than amorphous carbon, which in turn causes the varying catalytic activity and stability of the catalyst.

Matsukata et al.[39,40] studied the CH_4 reforming with CO_2 by stepwise method and found that two types of carbon formed on the Ni catalysts, filamentous carbon having a graphitic structure that could be gasified with CO_2 and mosslike carbon having an amorphous structure that was difficult to be gasified with CO_2.

5. Conclusion

The nature of catalyst support is found to significantly influence the catalytic activity of supported nickel catalyst in the reaction of methane reforming with carbon dioxide. The effect of support on catalytic performance can be ascribed to the aspects of the support structure, metal−support interaction, and acidity−basicity of support, affecting the metal dispersion and carbon deposition. The catalytic activities of the catalysts prepared in this work follow the order of $Ni/La_2O_3 \sim Ni/SiO_2 > Ni/\alpha\text{-}Al_2O_3 \sim Ni/MgO > Ni/CeO_2 > Ni/TiO_2$. The stability of catalysts is dependent on carbon deposition and metal sintering, and follows the order of $Ni/MgO > Ni/La_2O_3 > Ni/SiO_2 > Ni/\alpha\text{-}Al_2O_3 > Ni/CeO_2$. The high stability of Ni/MgO catalyst is attributed to the formation of solid−solid solution and more basic property, which leads to less reducibility and higher coking resistivity. Strong metal and support interaction results in a significant reduction in carbon formation on Ni/TiO_2 and Ni/CeO_2 catalysts. However, it causes site blockage resulting in lower catalytic activity and stability. Two kinds of carbon, amorphous and graphitic carbon, have been demonstrated to form on the surface of Ni catalysts and play different roles during the reaction.

Acknowledgment. We acknowledge the financial support by the Commonwealth Department of Education under the TIL program. We also thank Mr. F. Ausdley in the Department of Earth Science for conducting the XRD measurements and Mr. B. J. Wood, Department of Chemistry, for XPS measurements.

EF970092M

(38) Osaki, T.; Masuda, H.; Mori, T. *Catal. Lett.* **1994**, *29*, 33−37.

(39) Matsukata, M.; Matsushita, T.; Ueyama, K. *Energy Fuels* **1995**, *9*, 822−828.

(40) Matsukata, M.; Matsushita, T.; Ueyama, K. *Chem. Eng. Sci.* **1996**, *51*, 2769−2774.